Hardening and overaging Mechanisms in an Au-Ag-Cu-Pd alloy with In additions

Geon-Hoo Jeon, Yong Hoon Kwon, Hyo-Joung Seol, Hyung-Il Kim*

Department of Dental Materials, School of Dentistry and Medical Research Institute, Pusan National University, 1-10 Ami-dong, Seo-gu, Pusan 602-739, South Korea

Abstract

Hardening and overaging mechanisms were examined in a semi-precious Au-Ag-Cu-Pd dental alloy with small amounts of In, Zn and Ir. The alloy showed maximum age-hardenability at the aging temperature of 400°C. The hardness value increased to reach the maximum value, and then decreased continuously with aging time. In the early stage of aging process, the matrix of the single α_0 phase separated into the α_1 and AuCu I phases, and the fine InPd-based precipitates containing Zn and Cu formed at the grain boundaries. During further aging, the grain boundary precipitates grew toward the grain interior. In overaged specimens, the original matrix was replaced by the coarse lamellar structure composed of the AuCu I phase containing Pd and Zn and the Ag-Au-based α_1 phase of Cu-, Pd- and Zn-depleted. The hardness increase in the early stage of aging process was caused by the nucleation of the InPd-based phase and the AuCu I phase in the α_0 matrix; this introduced significant lattice strains into the interface with the matrix. The hardness decrease in the latter stage of aging process was caused by the formation and coarsening of the lamellar structure composed of the α_1 phase and the AuCu I phase. The minor constituent , In formed InPd-based grain boundary precipitates prior to the lamellar structure formation of α_1 and AuCu I.

Keywords

Dental gold alloy, Age-hardening, Phase transformation, X-ray diffraction, Scanning electron microscopy

1 Introduction

Low-melting elements such as In and Zn are known to improve the castability of dental alloys when added in small quantities. Such elements tend to form stable phases preferentially with Pd considered indispensable for dental alloys containing Ag. To promote tarnish and corrosion resistance these product phases may or may not contribute to the age-hardenability, one of the important properties essential for dental alloys. In the recent studies on the age-hardening mechanism of dental alloys, the Zn-containing InPd phase and the $(Pd,Ag)_3(In,Zn)$ phase were reported to be formed in the Ag - Pd - Au - In alloy with Zn and the Ag - Pd alloy with In, Zn and Ir, respectively (1,2). Both phases contribute to the hardness increase during aging process. Generally however, the phase composed of In and Pd may function differently, considering that the majority of dental alloys contain the Copper element the usual hardener.

In the present study, a Au-Ag-Cu-Pd alloy containing In, Zn and Ir as minor additions was used to examine the age-hardening and overaging mechanism. There have been several studies on the age-hardening behaviour of the Au-Ag-Cu-Pd alloys with or without minor additions (3-6). However, the phase transformation mechanisms vary with slight compositional changes during the aging process; therefore the product phases and their effect on the age-hardenability may alter with the variation of content of minor constituents. The object of this study is to identify the hardening and overaging mechanisms of a Au-Ag-Cu-Pd alloy containing small amounts of In, Zn and Ir by examining age-hardening behavior, and its relation with the phase transformations and changes in the microstructure and element distribution.

2 Experimental

2.1 Chemical composition of the alloy

The alloy used in the present study was a semi precious light yellow dental alloy used for crown and bridge fabrication (Goldenian C-47, Shinhung, Korea). The chemical composition of the alloy is listed in Table. 1. The alloy samples used were in the form of small square pieces 10 mm x 10 mm x 0.6 mm in a rolled and annealed condition.

2.2 Hardness testing

Before hardness testing, the alloy samples were solution-treated at 750°C for 10 min under an argon atmosphere, then rapidly quenched into iced brine to prevent any reaction occurring. Then samples were isochronally aged in the temperature range of 200°C to 500°C, and were isothermally aged at 350°C and 400°C for various periods of time in a

Table 1
Chemical composition of the alloy used

Composition	Au	Ag	Cu	Pd	In	Zn	Ir
wt%	47.5	36	10.6	4	1	0.7	0.2
at%	30.15	41.74	20.86	4.69	1.09	1.34	0.13

molten salt bath (25% KNO_3 + 30% KNO_2 + 25% $NaNO_3$ + 20% $NaNO_2$), used for the temperature range from 150°C to 550°C, then quenched into ice brine for subsequent hardness testing. Hardness measurements were completed using a Vickers micro-hardness tester (MVK-H1, Akashi Co., Japan) with a load of 300 gf and a dwell time of 10 s., All hardnesses being the average values of five measurements.

2.3 X-ray diffraction study

For the XRD study, the powder specimens at -300 mesh were produced by filing sample pieces . After being vacuum-sealed in a silica tube and solution-treated at 750°C for 10 min, they were isothermally aged at 400°C for various periods of time in a molten salt bath, and then quenched into ice brine. The XRD profiles were recorded by an X-ray diffractometer (D/Max-2400, Rigaku Denki Co. Ltd., Japan). The X-ray diffractometer was operated at 30 kV and 40 mA, and Nickel-filtered Cu Kα radiation was used as the incident beam.

2.4 Scanning electron microscopic examination

The samples were subjected to the required heat treatment, and then they were prepared by utilizing a standard metallographic techniques for SEM examinations to observe the microstructural changes in the specimen alloy during the aging process. A freshly prepared aqueous solution of 10% potassium cyanide and 10% ammonium persulfate was utilized for the final etching of the samples. The specimens were examined at 20 kV using a scanning electron microscope (S-2400, Hitachi, Japan).

2.5 Electron probe microanalysis (Epma) and energy dispersive spectrometer (Eds) analysis

EPMA and EDS analyses were completed to observe the distributional changes of each element in the specimen alloy during the aging process. For the EPMA and EDS analyses, the specimens were prepared as for SEM observations. An electron probe X-ray microanalyser (EPMA-1600, Shimadzu, Japan) and an energy dispersive X-Ray spectrometer (INCA x-sight, Oxford Instruments Ltd., UK) of field emission scanning electron microscope (JSM-6700F, JEOL, Japan) were used at 15 kV to examine the plate-like specimens.

3 Results and discussion

3.1 Hardness changes

Fig. 1 shows the isochronal age-hardening curves of the specimen alloy solution-treated at 750°C for 10 min, and then aged in the temperature range of 200°C to 500°C for 10 min and 20 min. The specimen alloy showed an apparent age-hardenability at the aging temperatures of 350°C and 400°C. Thus, the isothermal age-hardening curves were obtained at these various aging temperatures with aging time.

Fig. 2 shows the isothermal age-hardening curves of the specimen alloy solution-treated at 750°C for 10 min and then aged at 350°C and 400°C, respectively. The age-hardening rate was more rapid at 400°C due to the faster diffusion at higher temperature, but the age-hardening curves and age-hardenability were similar; this indicates that the same age-hardening mechanism supported at both aging temperatures.

In Fig. 2, the hardness increased drastically in the early stage of the aging process. At the aging time of 1 min at 350°C and 400°C, the hardness value increased up to approximately 90% of the maximum value; at longer times the rate of increase of hardness becameless . The maximum hardness value was obtained at the aging time of 50 min at 400°C and 500 min at 350°C, respectively, and then the hardness decreased continuously with aging time.

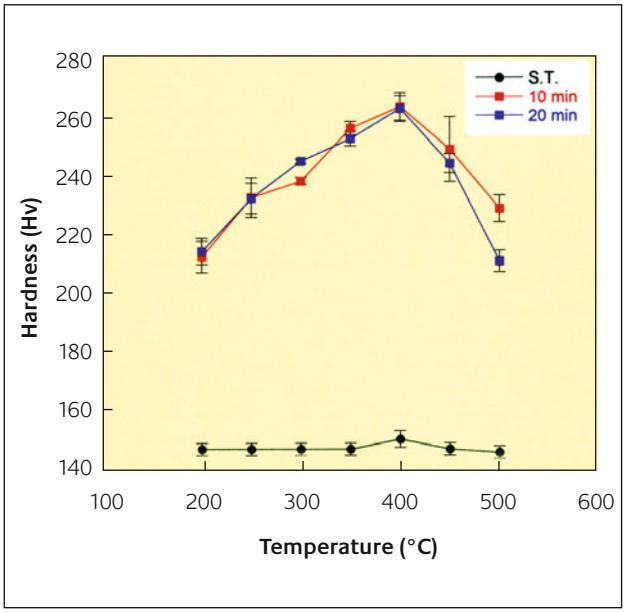

Figure 1
Isochronal age-hardening curves of the specimen alloy aged in the temperature range of 200°C to 500°C for 10 min and 20 min

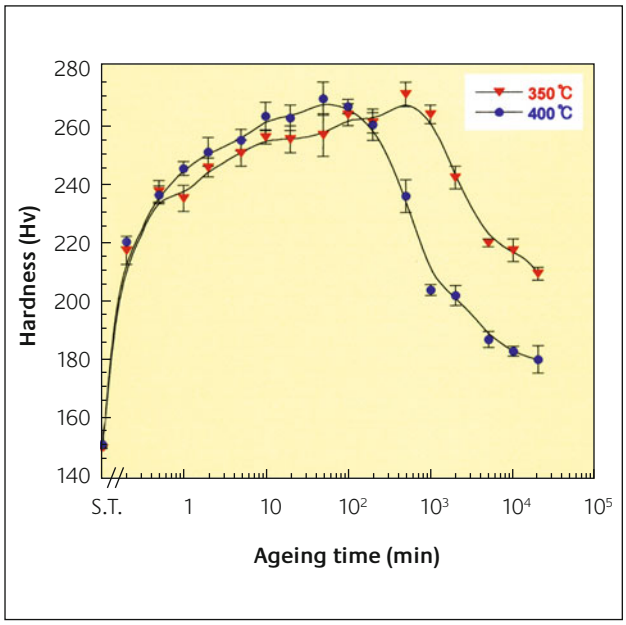

Figure 2

Isothermal age-hardening curves of the specimen alloy aged at 350°C and 400°C

3.2 Phase transformation

Fig. 3 shows the variations of the XRD pattern during the isothermal aging at 400°C with aging time. In the sample solution-treated specimen at 750°C for 10 min, the single face-centered cubic (f.c.c.) α_0 phase with a lattice parameter of a_{200} = 3.99 Å was obtained. By aging this sample at 400°C for 20000 min, the f.c.c. α_0 phase was transformed into the three phases of f.c.c., face-centered tetragonal (f.c.t.) and CsCl-type body-centered cubic (b.c.c.) structures. The f.c.c. phase of the strongest peak intensity was analyzed to be the Ag-Au-based α_1 phase with a little increased lattice parameter, a_{200} = 4.07 Å, compared to that of the α_0 phase. The f.c.t. phase among the product phases was analyzed to be the AuCu I phase with lattice parameters of a_{200} = 3.88 Å and c_{002} = 3.71 Å, which were a slightly different to the reported lattice parameters, a = 3.966 Å and c = 3.673 Å (7). Such a differences in lattice parameters were caused by the Pd and Zn contents in the product AuCu I phase, as it will be shown in Section 3.3. The CsCl-type b.c.c. phase among the product phases was analyzed to be the InPd-based phase with a lattice parameter of a_{110} = 3.20 Å. The reported lattice parameter of the InPd phase is a = 3.26 Å (7), and the Zn and Cu contents in the InPd -based phase of the specimen alloy resulted in the lattice parameter decrease, see Section 3.3.

In order to understand the relationship between the phase transformation and hardness changes, changes of the XRD pattern during the isothermal aging at 400°C were compared with the isothermal age-hardening curve. In Fig. 2, the hardness value increased up to about 90% of the maximum value at the aging time of 1 min at 400°C. In the corresponding XRD pattern, the intensity of the 111 α_0 peak decreased as the broad 111 α_1 peak appeared in the lower diffraction angle. The weak 110 peak of the InPd-based phase appeared in the higher diffraction angle of the 111 α_0 peak. The diffraction peaks of the AuCu I phase were not clear at this point. At the aging time of 10 min when the hardness value increased up to about 98% of the maximum value, the intensity of the 111 α_1 peak became stronger than that of the 111 α_0 peak, and the 111 peak of the AuCu I phase appeared to be obvious. The weak 110 peak of the InPd-based phase was wide and flat its peak position was located between the 111 peaks of the α_0 and AuCu I phases, adjacent them. At the aging time of 50 min when the maximum hardness value was obtained, the 111 α_0 peak almost disappeared, making the 110 peak of the InPd-based phase distinct. As the parent α_0 phase disappeared, the peak intensity of the product phases appeared stronger apparently except for the InPd-based phase.

During the period of the hardness decrease, the XRD pattern did not show any changes. The superlattice peaks of the AuCu I phase became obvious, however, at the aging time of 200 min when the hardness had decreased slightly. At the aging time of 20,000 min when the hardness decreased significantly by overaging, the XRD pattern did not change except for the peak sharpening of the peak.

From the above results, it was obvious that the increase in hardness occurred at the initial stage of the phase transformation of the α_0 phase into the α_1, AuCu I and InPd-based phases, and that the decrease in hardness occurred in the later stage of the phase transformation. In the XRD study, the broadening and subsequent sharpening of the diffraction peaks during the phase transformation corresponded to the increase and decrease in hardness, respectively. It is well known in studies of the age-hardening mechanism of dental alloys that the broadening of the XRD peak during the phase transformation indicates the introduction of lattice strains that cause the hardness to increase (8,9). From this it is clear

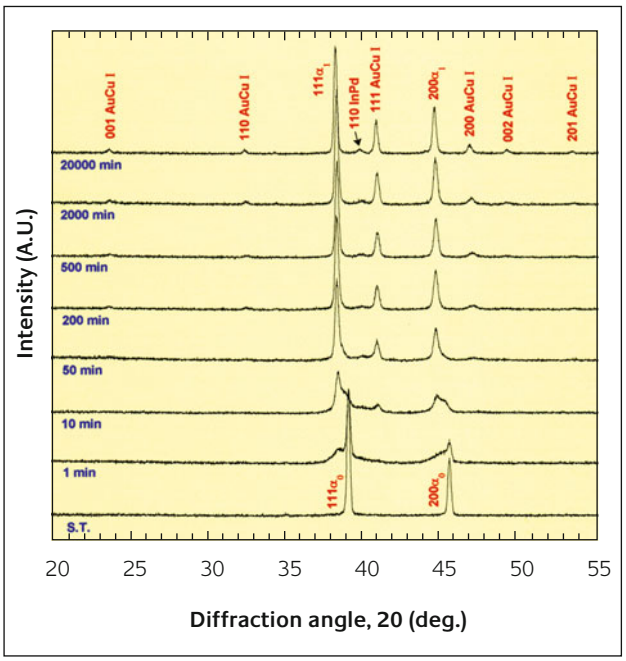

Figure 3

Variations of the XRD pattern during the isothermal aging at 400°C with aging time

that the significant lattice strains were introduced during the initial stage of the phase transformation of the α_0 phase into the α_1, AuCu I and InPd-based phases, and then the lattice strains were relieved continuously during the later stage of the phase transformation.

3.3 Element distribution

In order to examine the changes in the element distribution during the aging process, EDS analysis of FESEM and EPMA were completed. Fig. 4 shows the FESEM photographs for the specimens aged at 400°C for 50 min when the maximum hardness value was obtained (A) and 20,000 min when the hardness decreased significantly by overaging (B). The element distribution in the region marked by an arrow was analyzed with EDS of FESEM, and the results are shown in Table 2. In the specimen of the maximum hardness value (Fig. 4-A), the matrix composition (a) was close to the alloy composition of Table 1. At the grain boundary precipitates (b, c), the contents of Pd and In appeared to increased , and those of Zn were relatively rich. Even with the decrease in Au and Ag contents at the b- and c-regions, the Cu contents had not apparently diverged from that at the a-region (matrix). Considering the fine nature of the grain boundary precipitates, it is understandable that the EDS results at the b- and c-regions inevitably reflected the elements of the adjacent matrix to some extent. This and the XRD results of Fig.3 where the product phase of the weakest peak intensity had a slightly smaller lattice parameter than that of the reported InPd phase (7), the fine grain boundary precipitates seemed to be the InPd-based phase containing Zn and Cu. Although the matrix aged at 400°C for 50 min had a composition close to the alloy composition, it is obvious that the α_0 phase was separated into the product α_1 and AuCu I phases in the matrix from the XRD results of Fig.3 which showed that the parent α_0 phase disappeared.

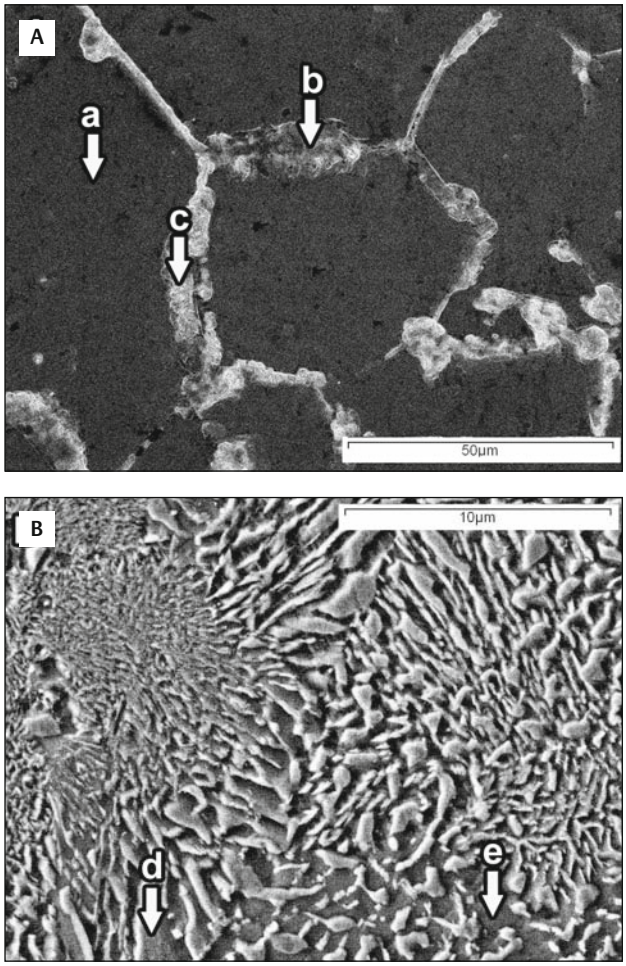

Figure 4
FESEM photographs for the specimens aged at 400°C for 50 min (A) and 20,000 min (B)

In the specimen overaged at 400°C for 20000 min (Fig. 4-B), the element distributionappeared to have changed. At the coarse precipitates (d), the decrease in Ag and increase in Cu were identified, but the content of Au was little changed. The Pd and Zn were relatively rich, but In was not detected. In the matrix (e) of the overaged specimen, the changes in distribution of Ag, Cu, Pd and Zn were the opposite of those at the coarse precipitates, that is, the increase in Ag and decrease in Cu were obvious, and Pd and Zn were relatively poor. In was detected as small amounts in the matrix of the overaged specimen, but the content of In seemed negligible compared to that at the grain boundary precipitates of the b- and c-regions.

Figs. 5 and 6 show the element distribution in the specimens solution-treated at 750°C for 10 min and aged at 400°C for 20000 min by the EPMA analysis. In the solution-treated specimen (Fig. 5), all the ingredients were contained homogeneously in the matrix. In the overaged specimen (Fig. 6), the matrix was separated into the Au-containing Ag-rich area and Au-containing Cu-rich area, and Pd was relatively

Table 2
EDS analysis for the specimens aged at 400 ˚C for 50 min (A) and 20,000 min (B) at the regions marked in Fig. 4

Region (at%)	Au	Ag	Cu	Pd	In	Zn	Ir
a	31.13	40.75	21.67	4.30	0.69	1.31	0.15
b	20.40	28.15	18.07	19.30	8.27	5.72	0.09
c	16.48	22.64	25.67	20.77	9.04	5.40	0
d	32.39	1.99	55.30	6.87	0	3.45	0
e	32.19	57.04	7.35	1.67	1.32	0.43	0

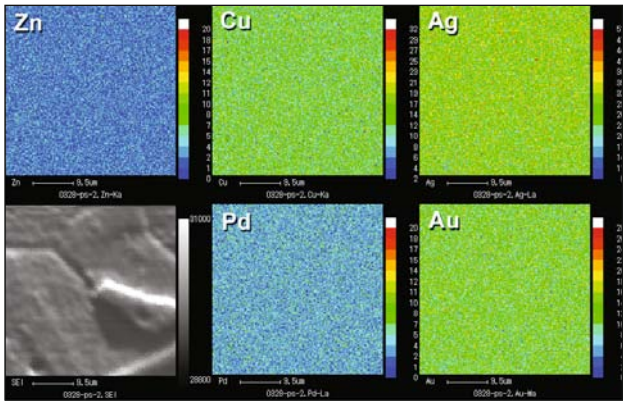

Figure 5

Element distribution in the specimen solution-treated at 750°C for 10 min by the EPMA analysis

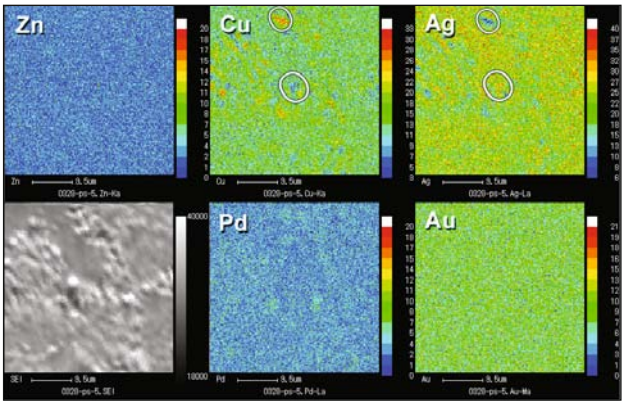

Figure 6

Element distribution in the specimen aged at 400°C for 20000 min by the EPMA analysis

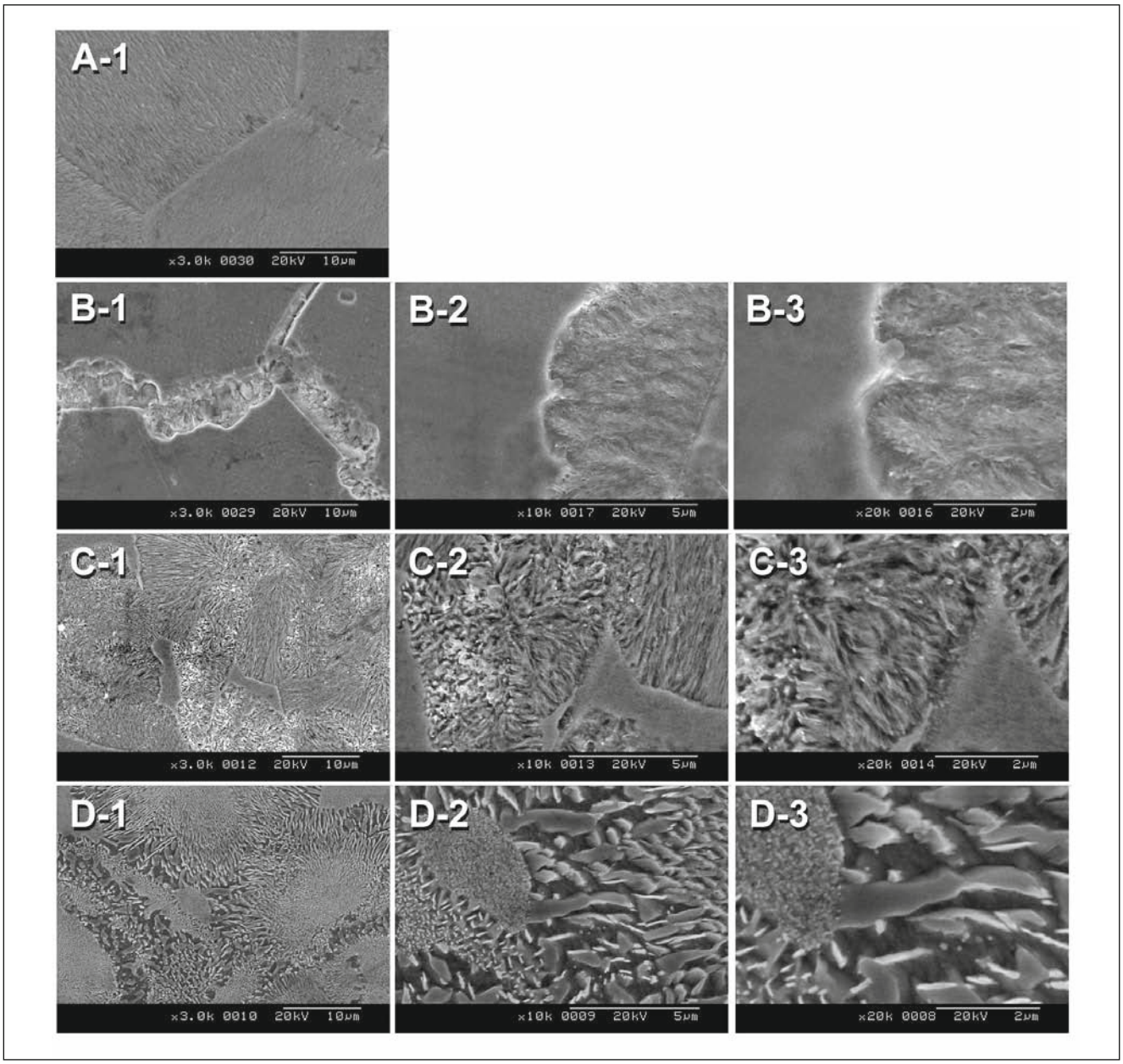

Figure 7

SEM photographs of 3000 (1), 10000 (2) and 20000 (3) magnifications for the specimens solution-treated at 750°C for 10 min (A) and aged at 400°C for 50 min (B), 500 min (C) and 20000 min (D)

rich in the Cu-rich area. The distribution of Zn and other minor constituents was undetectable by EPMA analysis. However, by considering the XRD, EDS and EPMA results together, it is clear that the matrix in the overaged specimen was composed of the Ag-Au-based α_1 phase of Cu-, Pd- and Zn-depleted, and the coarse precipitates were composed of the AuCu I phase containing Pd and Zn.

From the above results, we conclude that Ag and Cu were separated due to the solubility limit for each other during the aging process, while Au which has complete solubility in both elements was distributed homogeneously in the matrix (10). Accordingly, the lamellar structure composed of the AuCu I precipitates and the Ag-Au-based α_1 phase was formed in the matrix. The InPd-based precipitates were undetected in the overaged specimen by the EDS and EPMA analysis, but the XRD results (Fig. 3) proved its existence until the later stage of the aging process.

3.4 Microstructural changes

SEM examination was completed to determine the microstructural changes that are related to the hardness changes, . Fig. 7 shows the SEM photographs of 3000 (1), 10000 (2) and 20000 (3) magnifications for the specimens solution-treated at 750°C for 10 min (A) and aged at 400°C for 50 min (B), 500 min (C) and 20000 min (D). In the solution-treated specimen (Fig. 7-A), the matrix composed of the single α_0 phase was observed. By aging the specimen at 400°C for 50 min when the maximum hardness value was obtained (Fig. 7-B), the fine InPd-based precipitates were formed at the grain boundary. The changes in the matrix were not clear with SEM observations. It is obvious from the XRD results (Fig. 3), however that the α_0 phase was separated into the α_1 and AuCu I phases in the matrix, asdiscussed above. From this the hardness increase was thought to be caused by the nucleation of the InPd-based phase and the AuCu I phase in the α_0 matrix introducing apparent lattice strains in the interface with the matrix. The hardness increase by the nucleation of the InPd-based phase, however, seemed to be less effective than that by the AuCu I phase considering the much weaker peak intensity in the XRD pattern (Fig. 3).

At the aging time of 500 min when the hardness decreased by 10% of the maximum value (Fig. 7-C), almost the whole matrix except for the limited areas in the grain interior was replaced by the fine lamellar structure composed of the AuCu I precipitates and the α_1 matrix. Considering that the peak intensity of the InPd-based phase did not increase apparently with further aging, it is clear that the precipitates which spread broadly toward the grain interior did not comprise of the InPd-based phase, but the AuCu I phase.

By further aging for 20000 min (Fig. 7-D) when the hardness decreased significantly, the matrix was entirely replaced by the apparently coarsened lamellar structure composed of the AuCu I precipitates and the α_1 matrix. In the corresponding XRD pattern, the diffraction peaks became sharp and the superlattice peak intensity of the AuCu I phase increased. Considering such facts, it was thought that as the degree of AuCu I ordering increased with aging time and the growth and subsequent coarsening of the lamellar structure occurred to relieve the lattice strains in the interface between the precipitates and the matrix. This resulted in the continuous hardness decrease. The significant hardness decrease by the coarsening of the microstructure has been reported in dental alloys of various compositions (11, 12).

In the present study, the minor constituent , In, resulted in the formation of the InPd-based grain boundary precipitates in the early stage of aging process. If the formation of the InPd-based phase was prevented, the age-hardenability of the specimen alloy would be obtained only by the AuCu I phase formation which is the most well-known age-hardening mechanism in the majority of dental casting gold alloys. From the view point of tarnish and corrosion resistance, such additional phase formation by minor constituent is better prevented even though its contribution to the age-hardenability was approved. The InPd-based phase is stable in a wide temperature range from lower temperature (<-200°C) to 1285°C (10), and thus the elimination of In from the alloys may be reasonable to prevent the formation of the InPd-based phase during the aging process.

4 Conclusions

Hardening and overaging mechanisms of a semi-precious Au-Ag-Cu-Pd dental alloy containing In, Zn and Ir as minor constituents were examined, and the following results were obtained.

1. The hardness of solution-treated specimen increased drastically to the maximum value, and then decreased continuously with aging time.
2. When the maximum hardness value was obtained, the α_0 phase was separated into the α_1 and AuCu I phases in the matrix, and the fine InPd-based precipitates containing Zn and Cu were formed at the grain boundary.
3. By prolonged aging until the hardness decreased significantly, the matrix was replaced by the coarse lamellar structure composed of the AuCu I phase containing Pd and Zn and the Ag-Au-based α_1 phase of Cu-, Pd- and Zn-depleted.
4. The hardness increase in the early stage of aging process was caused by the nucleation of the InPd-based phase and the AuCu I phase in the α_0 matrix, and the hardness decrease in the later stage of aging process was caused by the formation and coarsening of the lamellar structure composed of the Ag-Au-based α_1 phase and the AuCu I phase.
5. The minor ingredient, In resulted in the formation of the InPd-based grain boundary precipitates prior to the formation and growth of the lamellar structure composed of α_1 and AuCu I.

About the authors

Geon-Hoo Jeon is currently working on research of dental gold alloys, Ph.D. in 2008.

Yong Hoon Kwon is associate professor of Department of Dental Materials, Ph.D. in 1997.

Hyo-Joung Seol is assistant professor of Department of Dental Materials, Ph.D. in 2003.

Hyung-Il Kim* is chairman of Department of Dental Materials, Ph.D. in 1989. On the editorial board of Dental Materials Journal (International Journal published by the Japanese Society for Dental Materials and Devices).

References

1 H.K. Lee, H.M. Moon, H.J. Seol, J.E. Lee, H.I. Kim, *Biomaterials,* 2004, **25**, 3869

2 Y.C. Suh, Z.H. Lee, M. Ohta, J. Mater. *Sci.: Mater. Med.*, 2000, **11**, 43

3 J.H. Lee, S.J. Yi, H.J. Seol, Y.H. Kwon, J.B. Lee, H.I. Kim, *J. Alloys Compd.*, 2006, **425**, 210

4 K. Hamasaki, K. Hisatsune, K. Udoh, Y. Tanaka, Y. Iijima, O. Takagi, S. Naruse, J. Mater. *Sci.: Mater. Med.*, 1998, **9**, 213

5 H.I. Kim, G.H. Jeon, S.J. Yi, Y.H. Kwon, H.J. Seol, *J. Alloys Compd.*, 2007, **441**, 124

6 H.I. Kim, M.I. Jang, B.J. Jeon, J. Mater. *Sci.: Mater. Med.*, 1997, **8**, 333

7 P. Villars, L.D. Calvert, '*Pearson's handbook of crystallographic data for intermetallic phases', American Society for Metals, Metals park*, 1985, pp. 1198, 2559

8 Y. Tanaka, K. Udoh, K. Hisatsune, K. Yasuda, *Materials Transactions, JIM.*, 1998, **39**, 87

9 H.J. Seol, T. Shiraishi, Y. Tanaka, E. Miura, K. Hisatsune, H.I. Kim, *Biomaterials*, 2002, **23**, 4873

10 T.B. Massalski, '*Binary Alloy Phase Diagrams', second ed., ASM International, Materials Park, OH*, 1990, pp. 12-13, 28-29, 358-360, 2271-2273

11 H.I. Kim, M.I. Jang, M.S. Kim, J. Oral. *Rehabil.*, 1999, **26**, 215

12 K. Hisatsune, Y. Tanaka, K. Udoh, K. Yasuda, J. Mater. *Sci.: Mater. Med.*, 1997, **8**, 277